



MONTE CARLO SIMULATION OF
“THERATRON EQUINOX 80” ^{60}CO
RADIOTHERAPY UNIT

By
MESAY GELETU GEBRE

SUBMITTED IN PARTIAL FULFILLMENT OF THE
REQUIREMENTS FOR THE DEGREE OF
MASTER OF SCIENCE IN PHYSICS

AT
ADDIS ABABA UNIVERSITY
ADDIS ABABA, ETHIOPIA
SEPTEMBER 2010

ADDIS ABABA UNIVERSITY
DEPARTMENT OF
PHYSICS

Supervisor:

Dr. ERMIAS GETE

Examiners:

PROF. A.K. CHAUBEY

DR. TATEK YERGOU

ADDIS ABABA UNIVERSITY

Date: **September 2010**

Author: **MESAY GELETU GEBRE**

Title: **MONTE CARLO SIMULATION OF “THERATRON
EQUINOX 80” ^{60}Co RADIOTHERAPY UNIT**

Department: **Physics**

Degree: **M.Sc.** Convocation: **September** Year: **2010**

Permission is herewith granted to Addis Ababa University to circulate and to have copied for non-commercial purposes, at its discretion, the above title upon the request of individuals or institutions.

Signature of Author

THE AUTHOR RESERVES OTHER PUBLICATION RIGHTS, AND NEITHER THE THESIS NOR EXTENSIVE EXTRACTS FROM IT MAY BE PRINTED OR OTHERWISE REPRODUCED WITHOUT THE AUTHOR'S WRITTEN PERMISSION.

THE AUTHOR ATTESTS THAT PERMISSION HAS BEEN OBTAINED FOR THE USE OF ANY COPYRIGHTED MATERIAL APPEARING IN THIS THESIS (OTHER THAN BRIEF EXCERPTS REQUIRING ONLY PROPER ACKNOWLEDGEMENT IN SCHOLARLY WRITING) AND THAT ALL SUCH USE IS CLEARLY ACKNOWLEDGED.

For my family and friends....

Table of Contents

Table of Contents	vi
List of Figures	vii
Abstract	x
Acknowledgements	xi
1 INTRODUCTION	1
1.1 Introduction	1
2 THEORY	5
2.1 Photon Interactions With Matter	5
2.2 Dosimetric Quantities in External Beam Radiotherapy	7
2.2.1 The depth of maximum dose (d_{max}) and percentage depth dose(PDD)	7
2.2.2 Relative dose factor (RDF)	9
2.2.3 Tissue Air Ratio(TAR)	10
2.2.4 Tissue-phantom ratio (TPR) and tissue-maximum ratio (TMR)	11
2.3 Monte Carlo Simulations in External Beam Radiotherapy	13
2.3.1 Fundamentals of the Monte Carlo Simulation	13
2.3.2 Review on Monte Carlo simulation of ^{60}Co Beam	14
2.3.3 BEAMnrc	17
2.3.4 DOSXYZnrc	19
3 MATERIALS AND METHODS	21
3.1 Modeling “Theratron Equinox 80” ^{60}Co Unit	21
3.1.1 “Theratron equinox 80” ^{60}Co radiotherapy unit	22
3.1.2 Source Capsule	22
3.1.3 The Collimation System	25

3.1.4	Main BEAMnrc inputs	27
3.1.5	EGSnrc electron / photon transport inputs	28
3.2	The Structure of Monte Carlo Simulation	28
3.2.1	The Structure of BEAMnrc Simulation	28
3.2.2	The structure of DOSXYZnrc calculation	30
4	RESULT AND DISCUSSION	31
4.1	Effects of field size on photon spectrum	31
4.1.1	Total photon spectra for different field size	31
4.1.2	Scattered photon spectra for different field size	33
4.2	Electron spectra for different field size	34
4.3	Percentage Depth Dose	35
5	CONCLUSION	37
	Bibliography	39

List of Figures

2.1	Geometry for PDD measurement and definition. Point Q is an arbitrary point on the beam central axis at depth d, point P is the point at d_{max} on the beam central axis. The field size A is defined on the surface of the phantom. The dose is measured at depth d and divided by the dose measured at d_{max}	8
2.2	PDD curves in water for a 10 x 10 cm ² field at an SSD of 100 cm for various mega voltage photon beams ranging from ⁶⁰ Co γ -rays to 25 MV X-rays.	8
2.3	Geometry for the measurement of the $RDF(A, hv)$. The dose at point P at z_{max} in a phantom is measured on a field with size A in part (a) and on a 10 x 10 cm ² field in part (b)	10
2.4	Geometry for measurement and definition of TAR. (a) The dose D_Q is determined at point Q in a water phantom; (b) the dose to small mass of water in air D'_Q is determined at point Q. Point Q is at the machine isocentre at a distance SAD from the source. The beam field size S_Q is defined at depth z in the phantom.	11
2.5	Geometry for measurement of $TPR(z, A_Q, hv)$. (a) The geometry for the measurement of D_Q at depth z in a phantom; (b) the geometry for the measurement of D'_{Qref} at depth z_{ref} in a phantom. The distance between the source and the point of measurement, as well as the field size at the point of measurement, is the same for (a) and (b).	12

2.6	Steps involved in using BEAMnrc system. To “specify ”an accelerator means to define an order set of component modules (CMs) to be used in the simulation. To build an accelerator consists of gathering all the source code, automatically editing, it to avoid duplicate names and compiling the resulting MORTRAN and FORTRAN code. To do simulation BEAMnrc reads in cross-section data set [prepared by the PEGS package from the EGSnrc system] [6] and input file which contains all the information related to that specific run: the complete geometry; the initial beam; the output required from this run; and the simulation control parameters. BEAMnrc outputs phase space data and graphics if requested and produces an output listing. The phase space data can be re-used.	20
3.1	The picture of “Theratron equinox 80 ” ⁶⁰ Co radiotherapy unit.	23
3.2	A cutaway diagram of the “Theratron equinox 80” ⁶⁰ Co unit source head. It shows the source capsule, source housing, and the two parts of collimator’s assembly; the upper primary definer and the lower collimator’s of interleaved, adjustable jaws.	24
3.3	The source region model including the radioactive material, the surrounding iron capsule and lead shielding used to simulate the head part.	24
3.4	The model of “Therartron equinox 80 ” ⁶⁰ Co unit (source region, primary fixed collimator, secondary movable collimators,trimmer bars, air gaps and air slabs between trimmer bars and patient plane) for this study.	26
4.1	Photon energy spectra at the patient plane (SSD=80 cm) for two field sizes (10 x 10, 30 x 30 cm ²).	32
4.2	Photon energy spectra at the patient plane (SSD=80 cm) for two field sizes (15 x 15, 25 x 25 cm ²).	32
4.3	Photon energy spectra at the phantom surface: total scattered photon from different components of the therapy unit (excluding primaries), for two field sizes.(15 x 15, 25 x 25 cm ²)	33
4.4	Photon energy spectra at the phantom surface: total scattered photon from different components of the therapy unit (excluding primaries), for three field sizes(10 x 10, 20 x 20, 30 x 30 cm ²)	33

4.5	Energy spectrum of the electrons reaching at SSD = 80 cm for three field sizes (10 x 10, 20 x 20, 30 x 30 cm ²).	34
4.6	Energy spectrum of the electrons reaching at SSD = 80 cm for three field sizes (5 x 5, 15 x 15, 25 x 25 cm ²).	35
4.7	Monte Carlo calculation result of percentage depth dose compared with measurement for 10 X 10 cm ² field size.	36
4.8	Monte Carlo calculation result of percentage depth dose compared with measurement for 20 x 20 cm ² field size.	36

Abstract

The BEAMnrc Monte Carlo package is used to simulate the ^{60}Co beam from the “Theratron Equinox 80” ^{60}Co radiotherapy unit. In modeling the ^{60}Co unit a particular attention has been paid for the geometry and material construction of the ^{60}Co source capsule, source housing, and the collimator assembly. The influence of field size on total photon spectra, scattered photon and electron spectra, (which is produced from the photon interaction with the materials surrounding the Cobalt source and collimator assembly), at the phantom surface (SSD equal to 80 cm) are studied. From our simulation the variation of total photon and scattered photon spectra with increasing field size is caused by scattered photons from different parts of the ^{60}Co radiotherapy unit. We also used BEAMnrc generated phase space files as beam source for DOSXYZnrc to calculate the percentage depth dose and compared with measured values.

Acknowledgements

Above all, I thank God for all He has done for me.

Any thesis, no matter how individualized, will almost certainly require input, assistance or encouragement from others; my theses is not exception.

I extend my sincerest gratitude to my advisors Dr. Mulugeta Bekele and Dr. Ermias Gete. They have been a constant source of thoughtful guidance in pursuing this thesis. Because of their input, advice and challenge, I have matured as a researcher and as a student. I would also like to acknowledge the contribution of Addissu Gezahegn, Semahegn Abayneh, Melakeselam Assefa and members of radiography and radiotherapy staffs at Black Lion Hospital.

I would also like to take this opportunity to express my strongest thank to my classmates and all my friends for their constructive suggestions and helpful comments. I thank Merkeb Berehanu for her help. Special thanks go to my family, and mostly Mom and Dad; they have definitely been encouraging me. They will always be dear to my heart.

I am also thankful to Asheber Gogile for his patient support in collecting and sending me my salary for entire two years.

Chapter 1

INTRODUCTION

1.1 Introduction

Medical physics is an applied branch of physics concerned with the application of the concepts and methods of physics to medicine or health care profession, which includes diagnosis, management, and treatment of human disease. One of the main area of application for medical physics is radiation therapy (radiotherapy). Radiotherapy is treatment of cancer by ionizing radiation. It is one of the major modalities of cancer treatment and every alternate cancer patient will require radiation during the course of treatment. There are two types of radiotherapy: (I) internal radiation therapy, also known as brachytherapy, in which the treatments involve placing radioactive materials encased in wires, seeds or small rods inside or adjacent to tumor site (II) external beam radiation therapy or teletherapy is the treatment where the radiation source is kept outside the body and the radiation beam is directed on to the tumor during treatment.

External beam radiotherapy is carried out mainly with three types of equipment that produces either X-rays or electrons: X-ray machines (superficial and orthovoltage), Linear accelerators (LINACs) which produces high energy electrons or high-energy X-rays for treatment of deep-seated tumors, and radioisotope machines that use high energy γ -emitting radioisotopes, such as Cobalt-60 and Cesium-137. The radioisotope machines are also referred to as Teletherapy Machines.

In External Beam radiotherapy, the radiation source is typically kept at a distance of 80-100 cm from the tumor to be treated. Cobalt-60 is the most widely used radioisotope, in teletherapy machines, due to the relatively high energy of the emitted photons, its long half-life, and its high specific activity. The use of ^{60}Co sources for teletherapy begun in the 1950s as a replacement of the 250 kVp X-ray treatment machines that were then in common use. Cobalt-60 has a half-life of 5.3 years and emits high energy (1.17 and 1.33 MeV) γ -rays. Today, however, in the developed world, linear accelerators have largely replaced radioisotope units for external beam radiotherapy because of their versatility and because of their sophisticated beam delivery system that allows for advanced treatments such as Intensity Modulated Radiotherapy (IMRT).

Although linear accelerators offer superior beam characteristics and faster treatments, these units are expensive and complex. In developing countries, the ^{60}Co unit is viewed as an indispensable tool for External Beam Radiotherapy because of its effectiveness, and its simplicity and dependability. In addition to the low cost of maintaining Cobalt-60 machines compared to LINACs, Cobalt-60 offers an entirely predictable output that is totally unaffected by temperature, humidity, power supply or other external influences. The major components of the ^{60}Co teletherapy machine are: a radioactive source; a source housing, including beam collimator and source movement mechanism; a gantry and stand in isocentric machines or a housing support assembly in stand-alone machines; a patient support assembly; and a machine console. A typical teletherapy ^{60}Co source is a cylinder of diameter 1.5 cm. to 2 cm., and is positioned in the treatment head with the circular end facing the patient.

In radiotherapy the amount of radiation given to the patient has to be accurately calculated so that the damage is limited to the cancerous cells only. Absorbed dose is one of the quantity that can be used to express the amount of radiation given to the patient, and most directly related to biological effects.

The SI unit of the dose is gray (Gy). It is seldom possible to determine the absorbed dose in most body tissues directly, and is usually determined by indirect means. One of the methods used to determine dose is to actually measure the dose in a “phantom”.

A phantom is a block of some material (usually water) that has the same radiation absorption properties as tissue, which is used to replace the patient during dose measurement. A dosimeter is inserted into the phantom and it is then exposed to radiation using known exposure factors. These measured dose values in the phantom can be used to calculate patient dose values by applying appropriate factors to account for different exposure conditions.

Even though the physics of photon and electron interactions in matter is well understood, in general it is impossible to develop an analytic expression to describe particle transport in a medium. This is because the electrons can create both photons (e.g., as bremsstrahlung) and secondary or knock-on electrons and conversely, photons can produce both electrons and positrons. In addition, both electrons and photons scatter. One widely used technique for solving this problem involves Monte Carlo simulation of radiation transport in which one uses knowledge of the probability distributions governing the individual interactions of electrons and photons in materials to simulate the random trajectories or histories of individual particles. Using Monte Carlo technique, it is possible to simulate the transport of radiation through a medium by sampling from known probability distributions for all possible interactions. Therefore, here we use Monte Carlo simulation to characterize the ^{60}Co photon beam from Theratron equinox 80” ^{60}Co radiotherapy unit.

G.Mora et al [9] used BEAM code to study about ^{60}Co beam from “Eldorado 6” radiotherapy unit. They calculated the central axis depth dose curve in water phantom, the scattered photon spectra from each component of the unit, and also studied the influences of the electron component on the total build up dose. For the present study, the

latest version of BEAMnrc Monte Carlo simulation package is used to model the “Theratron equinox 80” ^{60}Co radiotherapy unit. Using Monte Carlo simulation we wish to determine the energy spectra of the photons and the electrons at the patient plane for fixed source to surface distance(SSD) equal to 80 cm (we will try to investigate the effects of field size on the energy spectra of photons and electrons at the the patient plane). In addition we will calculate the dosimetric parameter percentage depth dose (PDD) for two different field sizes and compare these PDDs with measured values.

This thesis is organized as follows: In Chapter two we will discuss photon interactions with Matter, dosimetric quantities in external beam Radiotherapy, and we will give a review of the Monte Carlo method as it applies to model ^{60}Co beam. In addition we will give a literature survey of previous works in this area, and we will discuss briefly the BEAMnrc and DOSXYZnrc Monte Carlo package that was used in this study to model Theratron equinox ^{60}Co unit. In Chapter three we will describe, the Theratron equinox ^{60}Co radiotherapy unit, the geometric input that is used to model different parts of the ^{60}Co unit, the Monte Carlo radiation transport inputs of BEAMnrc and DOSXYZnrc, and finally the structure of Monte Carlo calculation for this study. In Chapter four we will present our Monte Carlo simulation results. The last chapter is concerned with the discussion and conclusion of this work.

Chapter 2

THEORY

2.1 Photon Interactions With Matter

Cobalt-60 decays with two gamma-rays lines at 1.17 and 1.33 MeV. As a photon passes through matter it can experience variety of interaction. For the energies stated above, the main interactions are photoelectric effect, Compton effect and pair production.

When the photon interacts via photoelectric effect, it transfers all its energy to an electron located in one of the atomic shells. The electron is ejected from the atom leaving a vacancy in the atom and begins to pass through the surrounding matter. Since the interaction creates a vacancy in one of the electron shells, typically the K or L, an electron moves down to fill the vacancy. The drop in energy of the filling electron produces a characteristic x-ray photon. In the photoelectric interaction some of the incident photon energy is utilized against binding energy of electron that is to make electron free. Therefore, this interaction will only occur if the energy of the incoming photon is greater than the binding energy of the electron. The energy E , of the ejected photo-electron will be,

$$E = hv - E_b \quad (2.1.1)$$

Where hv is the energy of the incident photon and E_b is the binding energy of the electron in the atom.

The photoelectric cross section varies with photon energy approximately as $(1/h\nu)^3$ and the coefficient per electron or per gram varies with atomic number approximately as Z^3 for high Z materials and nearly as $Z^{3.8}$ for low Z materials [18]

Compton interaction (incoherent scattering) is the interaction of the photon with a loosely bound electron in an atom. This interaction is one in which only a portion of the energy is absorbed and a photon is scattered with reduced energy. The kinetic energy, E , transferred to the free electron is given by,

$$E = h\nu - h\nu' \quad (2.1.2)$$

where $h\nu$ is the energy of the incident photon and $h\nu'$ is the energy of the scattered photon. Compton effect is much more important than either the photoelectric effect or pair production process for photons with energy (1.17 and 1.33 MeV) from Cobalt-60 decay. Compton interaction cross section is proportional to Z (atomic number) of the material and falls off as $1/h\nu$ [19]. Thus, the Compton cross section per unit mass is independent of the atomic number of the material

In Pair production the photon interacts with the field of the nucleus, is absorbed, and creates an electron-positron pair. A third body, usually a nucleus, is required to be present to conserve energy and momentum. The electron and the positron have the same mass, each equivalent to a rest mass energy of 0.51 MeV. Thus, this interaction occur only with photons with energies greater than 1.02 MeV. The resulting energy transferred to the electron-positron pair is,

$$E_+ + E_- = h\nu - 1.02MeV \quad (2.1.3)$$

Where $h\nu$ is the energy of the incident photon and E_+ and E_- are kinetic energies of positron and electron respectively. The pair production interaction cross-section is approximately proportional to Z^2 for different nuclei, and increases rapidly with energy above 1.02 MeV.

2.2 Dosimetric Quantities in External Beam Radiotherapy

2.2.1 The depth of maximum dose (d_{max}) and percentage depth dose(PDD)

For mega-voltage photon beams, the maximum dose (D_{max}) occurs at some depth from the surface, this is due to the build up phenomena. The depth in an irradiated medium, along the beams central axis, where the maximum dose (D_{max}) observed is the depth of maximum dose (d_{max}). It depends on the beam energy and beam field size. The beam energy dependence is the main effect, and d_{max} occurs more deeply for higher-energy beams; the field-size dependence is a minor effect. For the Cobalt-60 photon beam, d_{max} is 0.5 cm.

Percentage depth dose (PDD) is defined as the quotient, expressed as a percentage, of the absorbed dose at any depth d to the absorbed dose at a fixed reference depth d_{max} , along the central axis of the beam (see Figure 2.1).

Mathematically, PDD can be defined as:

$$PDD(z, A, f, hv) = \frac{D_d}{D_{max}} \times 100 \quad (2.2.1)$$

where D_{max} is the maximum dose, at depth d_{max} which is equal to 0.5 cm for the Co-60 photon beam, D_d is the dose at any depth and A is the field size on the surface.

Figure (2.2) shows a series of PDD curves for various mega-voltage photon beam. For all energies the PDD decreases with depth beyond d_{max} , however there is a region between the surface and d_{max} which is known as the dose build-up region in which the PDD increases with depth. The reason is that, with high energy photons, the electrons set in motion by photon interactions are projected primarily in the forward direction; hence, the number of electron tracks will increase with depth until a depth equal to the electron range is reached[18].

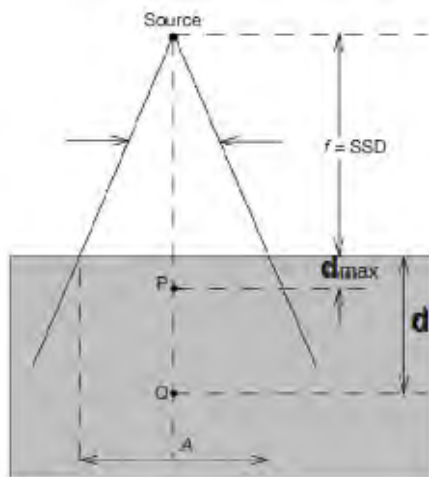


Figure 2.1: Geometry for PDD measurement and definition. Point Q is an arbitrary point on the beam central axis at depth d , point P is the point at d_{max} on the beam central axis. The field size A is defined on the surface of the phantom. The dose is measured at depth d and divided by the dose measured at d_{max} .

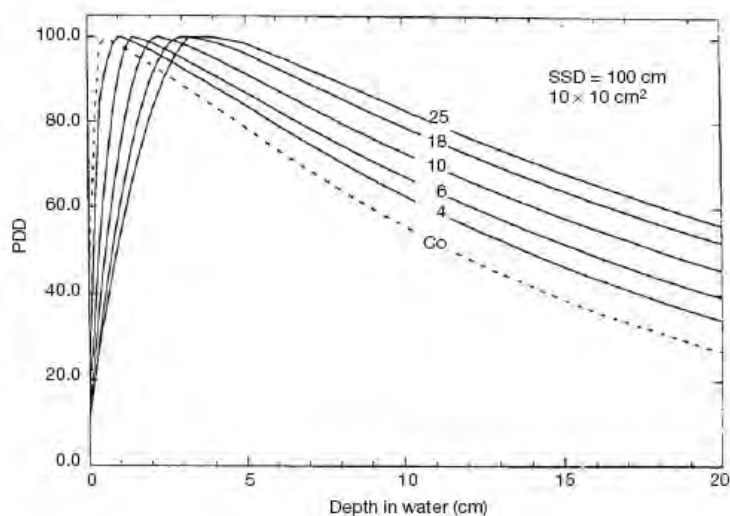


Figure 2.2: PDD curves in water for a $10 \times 10 \text{ cm}^2$ field at an SSD of 100 cm for various mega voltage photon beams ranging from ^{60}Co γ -rays to 25 MV X-rays.

From this point on the dose decreases with depth due to the attenuation of photon radiation. The result is that the PDD first increases with depth and then decreases.

2.2.2 Relative dose factor (RDF)

At a given SSD the dose at some point P depends on the field-size. One of the quantities used to characterize this dependence is relative dose factor (RDF). The relative dose factor (RDF) is defined as the ratio of $D_p(z_{max}, A, f, hv)$, the dose at P in a phantom for field A, to $D_p(z_{max}, 10, f, hv)$, the dose at P in a phantom for a 10 x 10 cm² field [17]:

$$RDF(A, hv) = \frac{D_p(z_{max}, A, f, hv)}{D_p(z_{max}, 10, f, hv)} \quad (2.2.2)$$

The relative dose factor (RDF) of a beam describes the photon scatter from all components of the head of the external beam radiotherapy as well as the scatter induced as the beam passes through the medium. The geometry for measurement of the $RDF(A, hv)$ is shown in Fig. 2.3 (a) for the measurement of $D_p(z_{max}, A, f, hv)$ and in (b) for the measurement of $D_p(z_{max}, 10, f, hv)$.

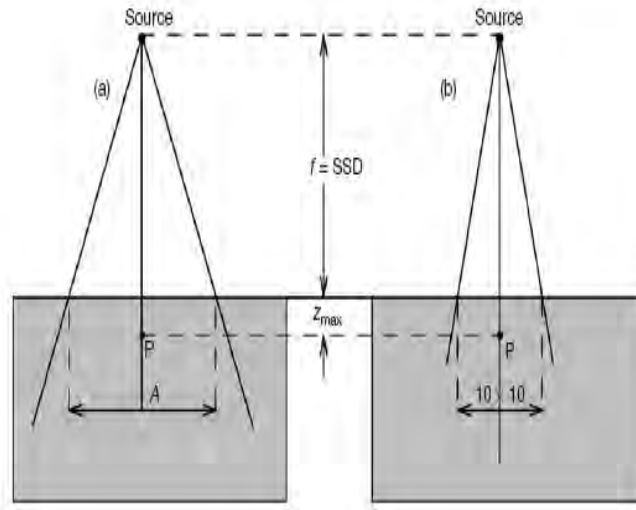


Figure 2.3: Geometry for the measurement of the $RDF(A, hv)$. The dose at point P at z_{max} in a phantom is measured on a field with size A in part (a) and on a $10 \times 10 \text{ cm}^2$ field in part (b)

2.2.3 Tissue Air Ratio(TAR)

TAR is defined as the ratio of the dose D_Q on the central axis in the patient or phantom to the dose D'_Q to small mass of water in air, at the same point Q on the beam central axis:

$$TAR(z, S_Q, hv) = \frac{D_Q(z, S_1, f)}{D'_Q(f + z, S)} \quad (2.2.3)$$

TAR is a concept which was developed to account for the attenuation and scatter in a phantom as a function of depth compared to a measurement free in air. It depends on depth z , the field size S_Q and energy of the radiation. TAR is independent of the distance from the source. The geometry for measurement of the $TAR(z, S_Q)$ is shown in Fig 2.4.

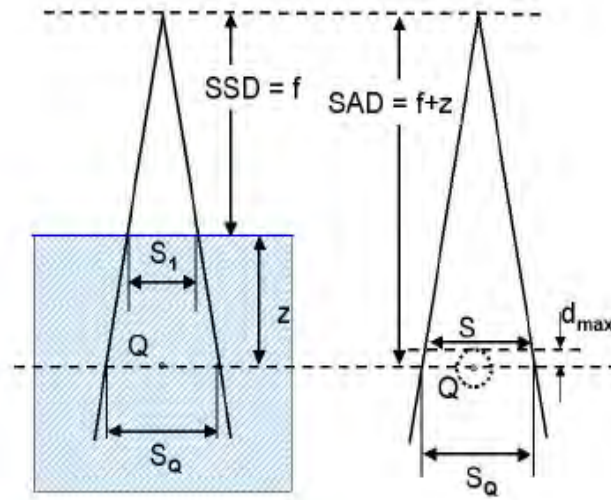


Figure 2.4: Geometry for measurement and definition of TAR. (a) The dose D_Q is determined at point Q in a water phantom; (b) the dose to small mass of water in air D'_Q is determined at point Q. Point Q is at the machine isocentre at a distance SAD from the source. The beam field size S_Q is defined at depth z in the phantom.

2.2.4 Tissue-phantom ratio (TPR) and tissue-maximum ratio (TMR)

The concept of TAR breaks down for higher energy beams because of difficulties in measuring the dose to small mass of water in air at these energies [17]. To solve this problem Tissue-phantom ratios were introduced as replacement for TAR for high energy radiations. The TPR is defined as:

$$TPR(z, A_Q, hv) = \frac{D_Q}{D'_{Qref}} \quad (2.2.4)$$

where D_Q is the dose in a phantom at arbitrary point Q on the beam central axis and D'_{Qref} is the dose, in a phantom at a reference depth z_{ref} (typically 5 or 10 cm) on the beam central axis. The geometry for the measurement of doses D_Q and D'_{Qref} is shown in Fig. 2.5. Similar to TAR, TPR depends on depth z, the field size A_Q and the energy hv it doesn't depend on the distance from the source.

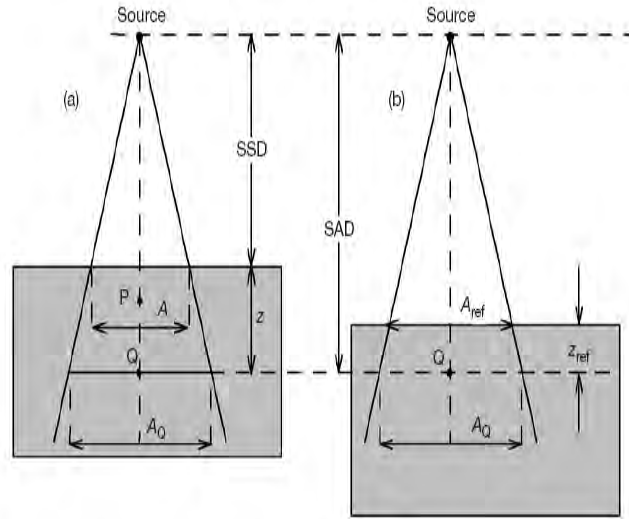


Figure 2.5: Geometry for measurement of $TPR(z, A_Q, hv)$. (a) The geometry for the measurement of D_Q at depth z in a phantom; (b) the geometry for the measurement of D'_{Qref} at depth z_{ref} in a phantom. The distance between the source and the point of measurement, as well as the field size at the point of measurement, is the same for (a) and (b).

If D'_{Qref} is measured at the reference depth z_{ref} equal to the depth of dose maximum z_{max} , a special TPR which is referred as the tissue-maximum ratio (TMR) defined:

$$TMR(z, A_Q, hv) = \frac{D_Q}{D'_{Qmax}} \quad (2.2.5)$$

where D_Q is the dose at point Q at a depth z in a phantom and D'_{Qmax} is the dose, at point Q at z_{max} . The geometry for the definition of TMR is the same as in Fig. 2.5, except that z_{ref} is now z_{max} .

2.3 Monte Carlo Simulations in External Beam Radiotherapy

2.3.1 Fundamentals of the Monte Carlo Simulation

“Monte Carlo method is a numerical solution to a problem that models objects interacting with other objects or their environment based upon simple object-object or object-environment relationships ” [19]. It has a wide range of application in radiation dosimetry and radiotherapy physics. In the context radiation transport, Monte Carlo techniques are those which simulate the random trajectories of individual particles by using machine-generated (pseudo-) random numbers to sample from probability distributions governing the physical processes involved. The physical processes occurs according to known probability functions, which are sampled using random numbers generated by computer routines.

As discussed above, Monte Carlo simulation requires the use of random numbers for generating a given probability distribution. This requires a random number generator (RNG) capable of producing a sequence of truly independent random numbers. Therefore, the random number generator (RNG) is the heartbeat of a Monte Carlo simulation system. Computers cannot provide a truly random sequence of numbers, but can calculate pseudo random sequences that are acceptable for most Monte Carlo applications. Nowadays, there are highly sophisticated computer codes that can generate a sequence of random numbers with a period of up to 2×10^{43}

In general Monte Carlo simulation system used in radiotherapy must be able to transport a particle through a medium by simulating all the physical interactions that the particle will encounter. The transporting medium will usually have an intricate geometry such as the head of external beam radiotherapy unit or a patients anatomy. When simulating an external photon beam, photons and a small number of particles are transported out of the radiotherapy unit head and until they encounter a volume of interest.

2.3.2 Review on Monte Carlo simulation of ^{60}Co Beam

The use of Monte Carlo for medical physics application has been reviewed by Mackie (1990) and Andreo (1991). Today, the Monte Carlo simulation has become the golden standard for absolute dosimetry, dose calculation and patient-specific dosimetric verification for radiotherapy. This expanded utilization is due to the availability of computing power and the accessibility of software packages such as DOSXYZnrc and BEAMnrc. There are several MC codes that have been used for modeling of radiotherapy beams. These are ETRAN/ITS, EGS4 , EGSnrc [6], MCNP4, PENELOPE and, most recently, GEANT3 and GEANT4 .

EGSnrc[6] is a general package for the Monte Carlo simulation of coupled electron-photon transport. EGSnrc Simulates radiation transport of electrons, positrons and photons through a medium in the energy range of 1 keV to several thousand GeV. The physics simulation is performed by a structured set of subroutines written in a language called MORTRAN. The EGSnrc transport code has been used in developing several simulation packages for applications in dosimetry of ionizing radiation: Linac Head simulation with BEAMnrc; patient dose calculation with DOSXYZnrc; calculation of dosimetric parameters(for example SPRZnrc for spectrum-averaged stopping power calculation, FLUZnrc for fluence calculation)

Several researchers have done a modeling of ^{60}Co teletherapy treatment unit using Monte Carlo simulation. Han et al. [12] used the EGS Monte Carlo code to compute the photon energy spectra, and to study the effect of changing the field size on output and on the dosimetric parameters such as PDDs and tissue-air ratio (TARs) from Theratron 780 Cobalt-60 unit. They computed the photon energy spectrum reaching the surface of the patient for a fixed source-to-surface distance (SSD). It is known that the energy spectrum consists not only of the 1.17 and 1.33 MeV primary photon lines, but also of a broad distribution of photons of lower energies resulting mainly from Compton interactions. They

concluded that the observed increase in output of the cobalt-60 machine with increasing field size is caused by scattered photons from the primary definer and the adjustable collimator of the unit. These spectra were then used as input to a pencil-beam model to calculate tissue-air ratios in water. The result was compared with a calculation that assumes a monochromatic photon energy of 1.25 MeV and measured data. The agreement among the three TAR curves was good up to a depth of 10 cm. Beyond that point, the dose contribution calculated for 1.25 MeV photons was higher than the dose calculated using a more realistic spectrum. This discrepancy is may be because, they used parallel beams, while for the measured data the beam is divergent. However, the significance of electron contamination could not be studied.

Rogers et al [11] studied electron contamination of an AECL ^{60}Co teletherapy source. To model the source they used EGS Monte Carlo radiation transport system. They split their calculations into a simulation of the source capsule, and a simulation of the rest of the geometry. They used a variety of variance reduction techniques to achieve a few percent statistical uncertainty on the depth dose component due to electron contamination. The sources for electron contamination found were, the source capsule (most effective at close SSD), the collimators, and the air (most effective at large SSD). At 80 cm SSD, for a field size equivalent to $35 \times 35 \text{ cm}^2$, about 45 percent of the dose at d_{max} is due to contaminant electrons of which 22 percent come from the source capsule and air-generated electrons; 10 percent and 13 percent from electrons emerging from the outer and the inner collimators respectively. The major source of scattered photons was the source capsule itself and scattered photons contribute 18 percent of the maximum dose. The inner and outer collimators were found to increase the effect of photon scatter by about 1 percent and 4 percent, respectively.

Mora et al.[9] used the BEAM [10] Monte Carlo code to simulate the Cobalt-60 beam from an “Eldorado 6” radiotherapy unit and to calculate the relative air-kerma output

factors as a function of field size. This unit is more realistically modeled because the previous works modeled cylindrical symmetry about the beam axis and solid collimators instead of the complex leaves of the collimators structure, but this work used realistic rectangular geometry of the collimator assembly and simulates the collimator system using simplified model consisting of solid blocks of lead. The calculated relative air-kerma output factor at $SSD = 80.5$ cm agreed to within 0.1 percent with measured values. They were able to show that the variation of the output factor is almost entirely due to scattered photons from the fixed and adjustable collimator and there was no effect of shadowing primary photons. The influence of the geometry of the collimating system on the energy spectra of photon along central axis is shown to be small but finite. The calculated depth-dose curve in the buildup region in a water phantom irradiated by a narrow and broad Cobalt-60 beam is shown to agree with experimental data at 2 percent and 3 percent levels. Unlike prior calculations, their results accurately predicted the effect of electron contamination from the surface to dose maximum. The field size is shown to have some effect on the photon spectra.

Theratron 780-C, which is one of the most commonly used model of ^{60}Co teletherapy unit was modeled by Sichani and Sohrabpour [13]. The Monte Carlo transport code MCNP was used to simulate the photon beam from a Theratronics 780-C cobalt therapy unit and to calculate some dose-dependent parameters as functions of field size. The simulation has modeled the source capsule, collimators (fixed and adjustable), the lead shielding in the unit head, and the jaws as ranged from 5×5 to 35×35 cm². In their work the role of the unit head lead, as well as the fixed and the adjustable collimators and finally the field size effects on the production of the scattered photons had been studied. The various dosimetric parameters of PDD, PSF and TAR have been calculated. The dosimetric parameters have differences with the measured values were of the order of or less than 1 percent.

2.3.3 BEAMnrc

In 1995 the Monte Carlo simulation package BEAM code [10] was released for general use and has become very widely used for many research purposes. It is based on EGS4 Monte Carlo radiation transport code. BEAM was designed to model all types of radiotherapy accelerators (as well as ^{60}Co units and x-ray units). The model of the accelerator or radiotherapy unit is built from a series of component modules (CMs). A CM is a simple geometric shape, and varies from a simple slab to a complicated structure such as a multi leaf collimator. Each CM can be re-used several times to build different parts of the accelerator (eg the JAWS CM is used to model the jaws which limit the beam when used in photon beam mode and in the case of the electron beam the applicator is made of parallel bars. The surfaces of each CM are perpendicular to the axis of the accelerator. BEAM can have as an input, beams of electron, photons or positrons. BEAM handles a wide variety of input source geometries most of which are assumed to start at the top of the accelerator. There can be an arbitrary number of scoring planes which are at the back of the accelerator. The scoring planes are located at user specified distances from the given CM and are perpendicular to the beam axis.

The first step in modeling a particular radiotherapy machine is to “specify” the machine means to define an ordered set of component modules (CMs) to be used in the simulation. The second step is to “build” the machine, which consists of collecting all the source code, automatically editing to avoid duplicate names and compiling the result into MORTRAN and FORTRAN code. The final step is to compile and run or execute. To do simulation BEAM reads in cross-section data set [prepared by the PEGS package from the EGS4 system] [6] and input file which contains all the information related to that specific run: the complete geometry; the initial particle; the output required from this run; and the simulation control parameters. The primary output of simulation is a large file called phase space file which is scored at a given scoring plane. The phase

space contains information about all the particles that have crossed the scoring plane. For each particle, the phase space file contains the following information: the particle type, the co-ordinates at which the particle crossed the scoring plane, the momentum vector of the particle. The phase space file can be used as an input in further BEAM calculations.

The BEAMnrc, which is an improved version of BEAM, was developed as part of the OMEGA (Ottawa Madison Electron Gamma Algorithm) project to develop 3-D treatment planning for radiotherapy (with collaboration between NRC and the University of Wisconsin). BEAMnrc uses the EGSnrc Monte Carlo system of radiation transport that is built on the EGSnrc Code System. The transport physics in EGSnrc [6] is greatly improved over that in EGS4 (the basis for all BEAM versions). The component geometry, composition and relative positions of the all types of radiotherapy accelerators (as well as ^{60}Co units and x-ray units) components are constructed via a Graphic User Interface (GUI). Fig(2.6) shows steps involved in modeling the radiotherapy machine and simulating electron and photon transport with BEAMnrc.

To analyze the BEAMnrc phase-space data and to derive the spectral and planar fluence distributions for use by beam characterization models we used BEAMDP (BEAM Data Processor) [3, 4]. BEAMDP is used to analyze the phase-space parameters of a photon or electron beam generated using BEAMnrc and to derive the data required by a multiple-source model for representation and reconstruction of the electron beam for use in Monte Carlo radiotherapy treatment planning. Further more, BEAMDP can also be used as a utility program to derive other information about the simulated electron beams from their phase-space files. The graphical user interface BEAMDP GUI greatly facilitates running BEAMDP by not requiring the user to re- enter parameters from scratch every time when phase space data is analyzed.

2.3.4 DOSXYZnrc

DOSXYZnrc [2] is latest version of DOSXYZ code developed for the EGS4 code system and uses EGSnrc-based Monte Carlo simulation code for calculating 3-dimensional absorbed dose. DOSXYZnrc simulates the transport of photons and electrons in a Cartesian volume and scores the energy deposition in the designated voxels.

Since DOSXYZnrc requires an input file to be generated by the user, giving a complete description of the phantom and the source, the graphical user interface DOSXYZnrc GUI which allows input files to be created and executed graphically [4] is used. A variety of beams may be incident on the phantom, including full phase-space files from BEAMnrc. For all simulations here a water phantom is used as the patient geometry. The water phantom for dose calculations is simulated using the latest version of DOSXYZnrc.

An interactive program STATDOSE [8] is used for analyzing 3-dimensional dose distributions and for plotting 1-dimensional dose distributions using the xvgr/xmgr plotting package for 3-dimensional dose generated by DOSXYZnrc. STATDOSE functions include normalization, re- binning, plotting and analysis of the dose distributions.

Steps involved in simulating electron and photon transport with BEAMnrc

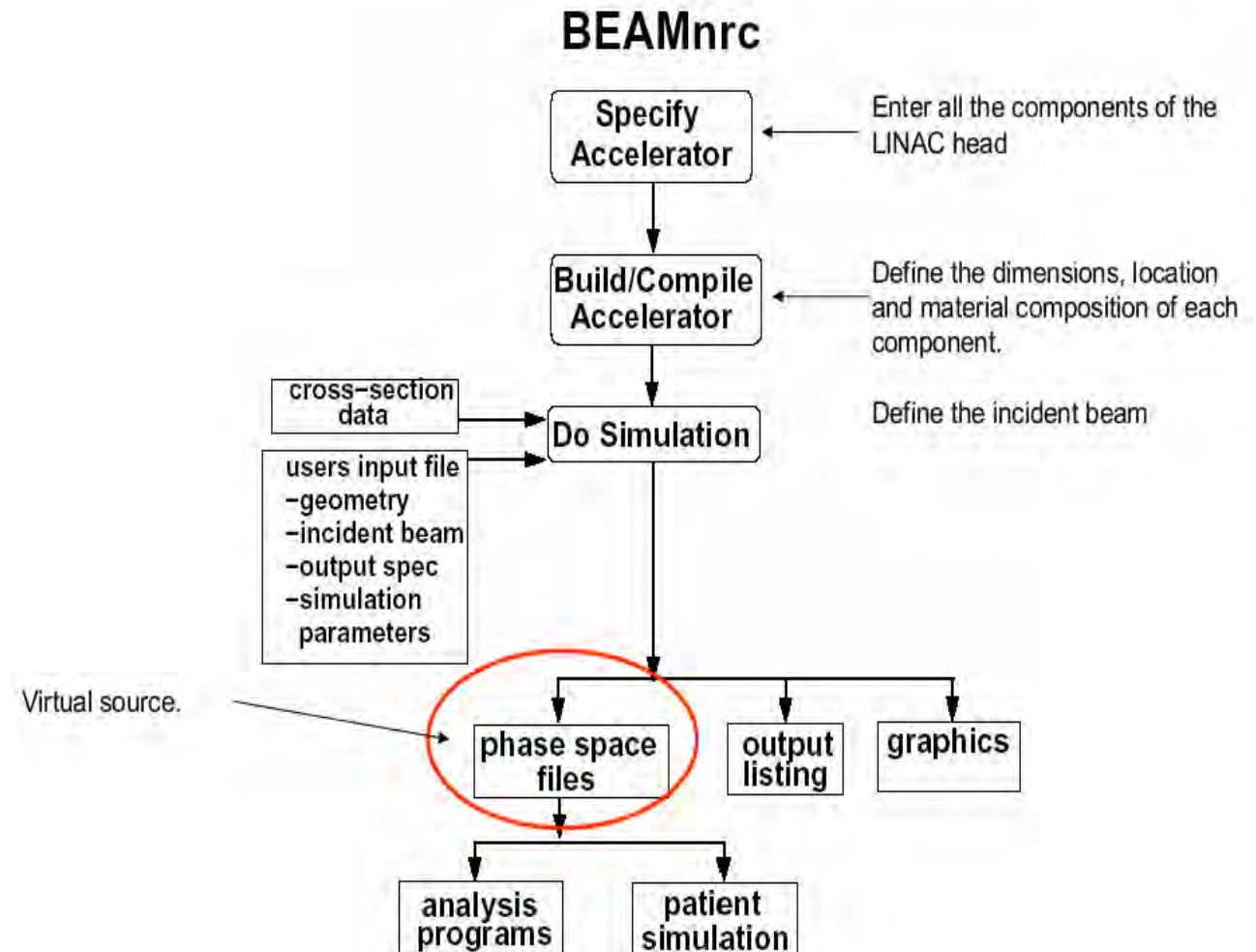


Figure 2.6: Steps involved in using BEAMnrc system. To “specify ” an accelerator means to define an order set of component modules (CMs) to be used in the simulation. To build an accelerator consists of gathering all the source code, automatically editing, it to avoid duplicate names and compiling the resulting MORTRAN and FORTRAN code. To do simulation BEAMnrc reads in cross-section data set [prepared by the PEGS package from the EGSnrc system] [6] and input file which contains all the information related to that specific run: the complete geometry; the initial beam; the output required from this run; and the simulation control parameters. BEAMnrc outputs phase space data and graphics if requested and produces an output listing. The phase space data can be re-used.

Chapter 3

MATERIALS AND METHODS

3.1 Modeling “Theratron Equinox 80” ^{60}Co Unit

The more recent Monte Carlo simulations of radiation transport code EGSnrc/BEAMnrc and the EGSnrc/DOSXYZnrc are used for this study. These codes have been widely used for the modeling of radiation therapy units (e.g. linear accelerators as well as ^{60}Co units and x-ray units) and for radiation therapy dose calculations [1], [2], [9], [12], [11].

In this work, “Theratron equinox 80” ^{60}Co radiotherapy unit is modeled with BEAMnrc [1]. All simulations were done using 64 processor HP cluster. In modeling this unit a particular attention is paid for modeling of the geometry and material construction of the ^{60}Co source capsule, the source housing, and collimator assembly. The unit has been realistically modeled: the cylindrical source capsule and its housing, the rectangular collimator system, the primary and secondary jaws and the air gaps between the components. To create the input files, the graphical user interface BEAMnrc GUIs [5] which were created to help the user in both creating and editing the input files by providing a label and a text box or option menu for each parameter, with a detailed explanation available in a help window is used. There is also added benefit in the BEAMnrc GUI which is the preview option for each CM and of the entire unit, where the user may look at a graphical representation of the CM or of the unit that he or she had defined.

3.1.1 “Theratron equinox 80” ^{60}Co radiotherapy unit

“Theratron equinox 80” ^{60}Co radiotherapy unit (manufactured by Theratronics) is used widely in many countries all around the world. It consists mainly of a source capsule, fixed collimator which is made of tungsten, adjustable collimators that are made lead and tungsten, and the lead shielding which is housed in the unit head. The various therapy treatment beam field sizes can be defined by means of the adjustable collimator, which consists of four sets of lead vanes and two trimmer bars. Fig (3.1) is a picture of the actual Theratron equinox 80 ^{60}Co radiotherapy unit and Fig(3.2) is cutaway diagram of the Theratron equinox 80 head, which shows the source capsule, source housing, and the two principal sections of the collimator assembly; the upper fixed primary definer and the lower movable secondary collimators.

3.1.2 Source Capsule

In modeling the source and the capsule of the ^{60}Co unit, the model used by Rogers, et al [9] is used. This model has cylindrical geometry about the beam axis. Although the real source of gamma radiation is made up of many small ^{60}Co pellets, the cylindrical source was modeled using, a vertical ring configuration centered on the Z-axis, “ISOURCE 3”: Interior isotropic cylindrical source with 2 cm diameter. This source can only be used inside CONESTAK, SIDETUBE or FLATFILT CMs. Here we used the CONESTAK CM which has cylindrical symmetry as a capsule to put “ISOURCE 3 ” inside it. The ‘bareCo60’ ^{60}Co source spectrum with 1.17 and 1.33 MeV mono-energetic gamma -photons was used in the simulations. Figure (3.3) is a diagram of the model of theratron equinox 80 ^{60}Co unit source region. Showing the placement, material used and dimensions of the active source, surrounding iron capsule, and lead shielding.



Figure 3.1: The picture of “Theratron equinox 80 ” ⁶⁰Co radiotherapy unit.

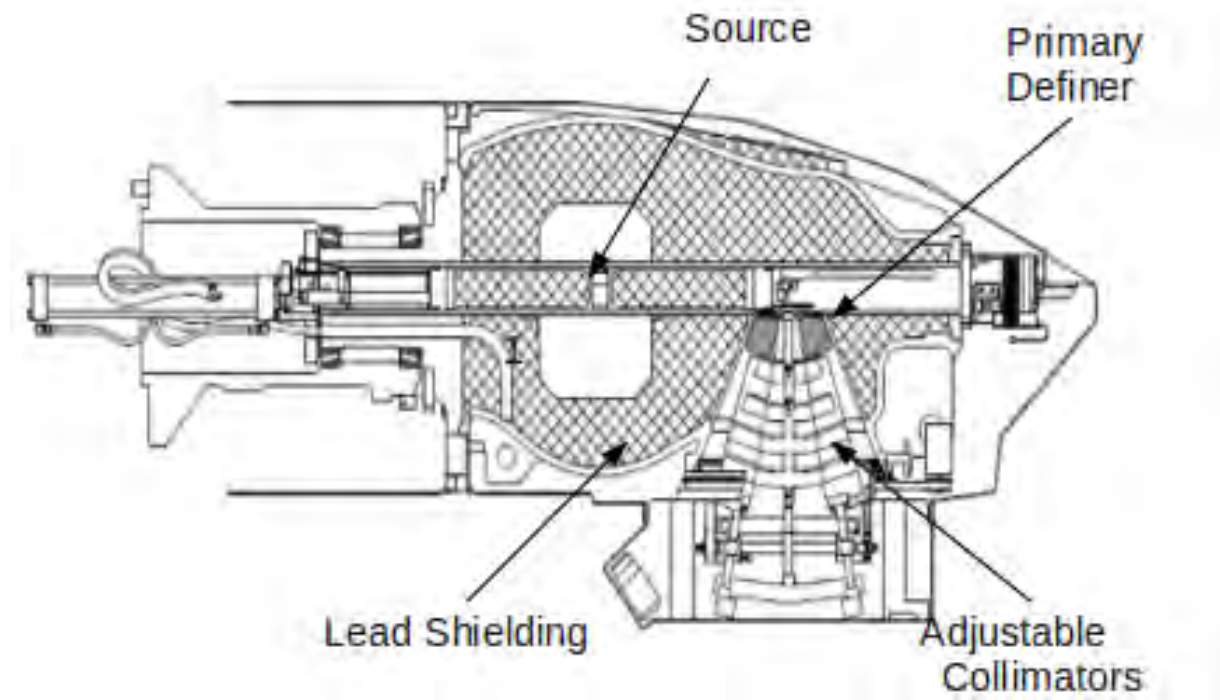


Figure 3.2: A cutaway diagram of the “Theratron equinox 80” ^{60}Co unit source head. It shows the source capsule, source housing, and the two parts of collimator’s assembly; the upper primary definer and the lower collimator’s of interleaved, adjustable jaws.

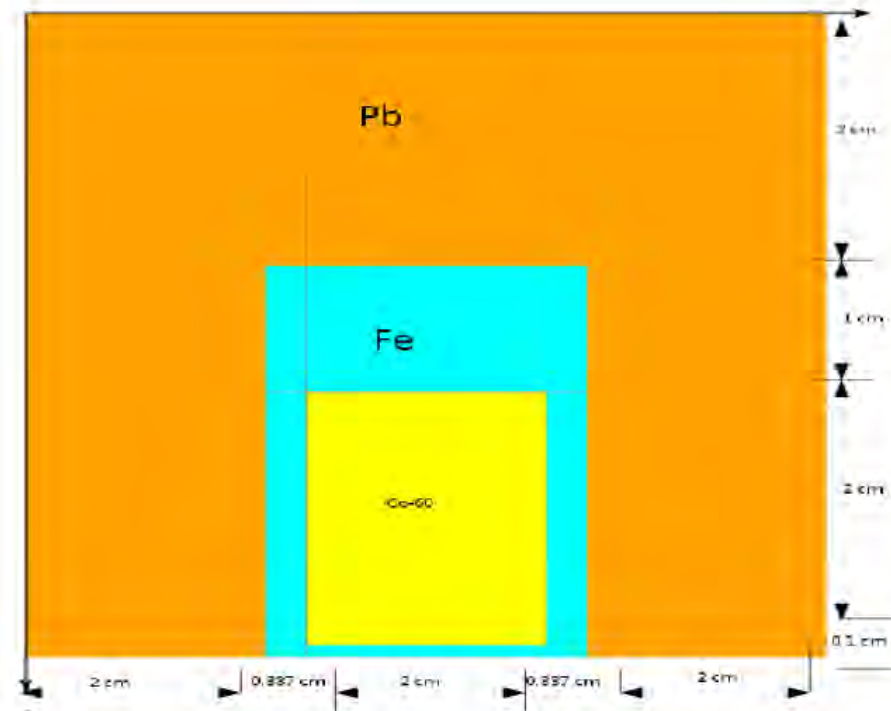


Figure 3.3: The source region model including the radioactive material, the surrounding iron capsule and lead shielding used to simulate the head part.

3.1.3 The Collimation System

To model the actual rectangular geometry of the collimator assembly the component module (CM) PYRAMIDS and JAWS are used with geometry data's of collimators of theratron 780 from Canada.

Just after 1.51 cm air gap from the capsule, the CM PYRAMIDS which is useful for modeling rectangular collimators and beam blocks is used to model a fixed primary collimator. This CM has a square outer boundary centered on the beam axis and it is made up of tungsten. The fixed collimator is 6.35 cm in length, and the inner and outer opening radii are 1.072 cm and 2.39 cm, respectively.

The inner movable secondary collimators, just 0.4 cm below the primary definer are simulated with the JAWS component module (CM) which is made up of lead. The actual adjustable collimator consisted of four sets of interleaved lead vanes. However, in the model, four sets of JAWS CM surrounded the beam on the same layer and the thickness of each layer in X and Y direction are, the first 2.62 cm, the second and third 2.064 cm each and the fourth 2.064 cm in Y and 1.67 cm in X direction. Then finally, the total thickness of inner collimators is 20.48 cm vertically with source face-collimator distance 7.86 cm. These adjustable collimators of teletherapy machine move in the xy-plane and are perpendicular to the beam direction to provide square and rectangular radiation fields typically ranging from 5 x 5 to 35 x 35 cm² at 80 cm from the source.

After the movable collimators, two trimmer bars upper and lower, that helps to minimize geometric penumbra which results from a finite source diameter, are simulated by component module (CM) JAWS with source face-trimmer bar (upper set) distance 39.62 cm. Each upper and lower trimmer bars thickness is 2.54 cm with 0.3 cm air gap and the distance from the source to the bottom of lower trimmer bar (SDD) is 45.0 cm.

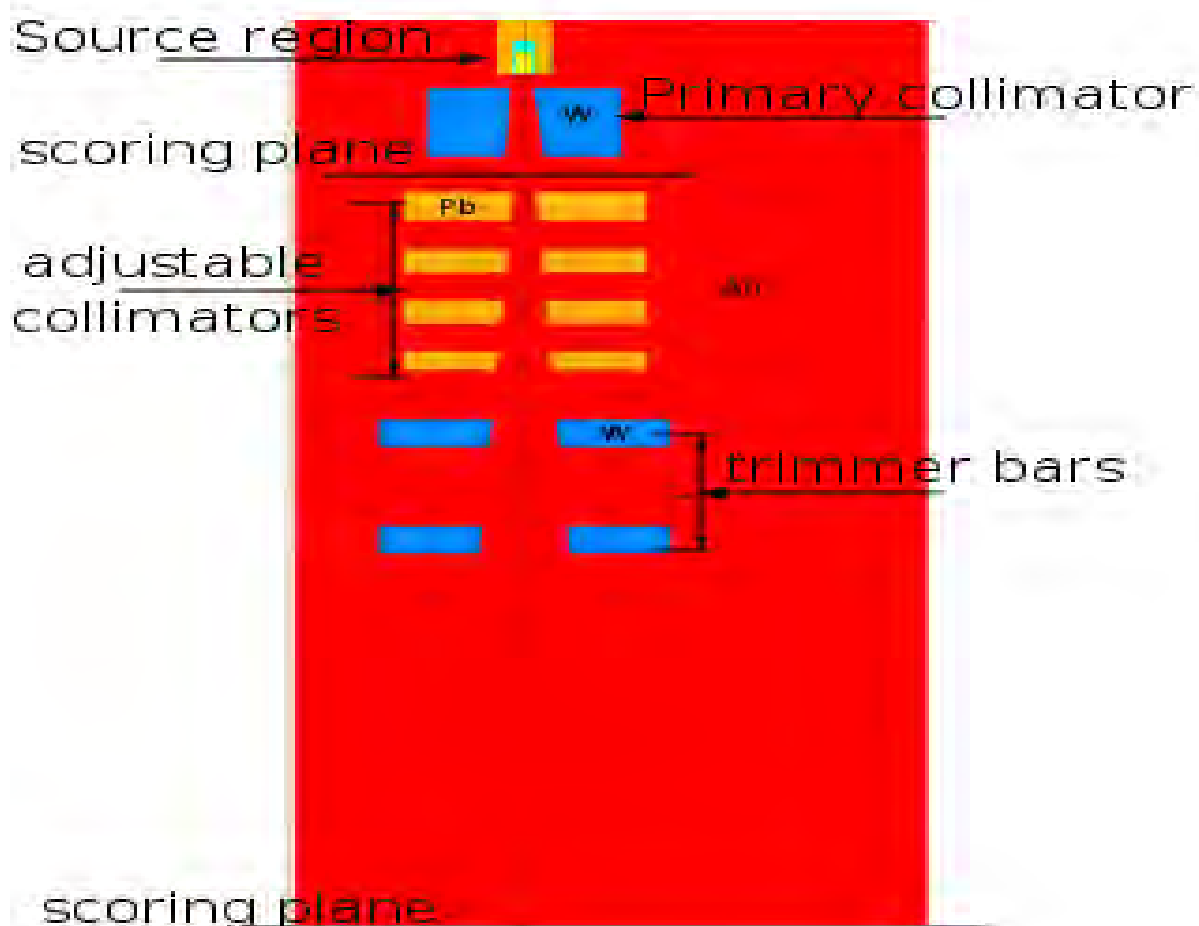


Figure 3.4: The model of “Theratron equinox 80 ” ^{60}Co unit (source region, primary fixed collimator, secondary movable collimators, trimmer bars, air gaps and air slabs between trimmer bars and patient plane) for this study.

This component is adjusted depending on the desired field size at 80 cm from the source. Between the bottom of lower trimmer bar and the patient plane, 35.0 cm thickness air slab (SLABS CM) is simulated. Figure (3.4) shows the model of Theratron equinox ^{60}Co unit in this study which includes the source head, the primary definer, secondary adjustable collimators, trimmer bars and the air slab between trimmer bars and scoring plane.

3.1.4 Main BEAMnrc inputs

Here we describe main BEAMnrc inputs for photon electron transport from the source to the scoring plane including efficiency improving techniques.

Since the variance on different quantities is directly related to the number of particles, in order to improve the accuracy of the calculations, more particle histories should be simulated (Francescon et al 2000). Therefore, to keep statistical error less than or equal to 2 percent, up to 2.0×10^9 and 6.0×10^9 histories were simulated for the DOSXYZnrc and the BEAMnrc simulations.

One of the major advantage of Monte Carlo technique in BEAMnrc is that it allows detailed information about each particle history to be known with Variable LATCH. So to store each particle history during a variable LATCH is used, so that we can determine from where a particle is scattered. That means whether from source region, primary definer, adjustable collimator or air slab. The central axis region and at the front or back of each CM is set to be air.

The use of the various variance reduction techniques were essential to achieve one or more objectives of obtaining a result, and speeding up of the calculations. To save a significant amount of CPU simulation time one of Variance Reduction technique in BEAMnrc called “Range Rejection of electrons” was used. Generally BEAMnrc stops tracking an electron if it can not get out of the present region with enough energy to reach the scoring plane. In addition the energy thresholds for electron and photon transportation, the global electron and photon cutoff energies (ECUT and PCUT) were set at 0.700 and 0.010 MeVs, respectively.

3.1.5 EGSnrc electron / photon transport inputs

EGSnrc, is a general purpose code for the Monte Carlo simulation of charged particle and photon transport through the medium [6]. The use of EGSnrc to simulate charged particle and photon transport in BEAMnrc allows the user a greater degree of control over the transport physics as compared to previously available EGS4 versions of BEAM. The next paragraph describes the EGSnrc inputs in this simulation.

EGSnrc transport parameters which are different from default setting are, Atomic Relaxations= On, Brems cross sections= NIST. The default Electron-step algorithm (transport algorithm) PRESTA-II which is the new, more accurate, algorithm developed for use with EGSnrc and default boundary crossing algorithm EXACT which was introduced in EGSnrc to eliminate a known fluence singularity caused by forcing a multiple scattering event at a boundary are set. Further more some other default settings are, maximum fractional energy loss/step (ESTEPE) was set at 0.25, photon cross sections was set to be “Storm-Israel” and Spin effects= on.

3.2 The Structure of Monte Carlo Simulation

3.2.1 The Structure of BEAMnrc Simulation

To save calculation time in BEAMnrc simulation of the full ^{60}Co therapy unit we split the calculation into three steps. The first two stages of BEAMnrc simulations, which are used to generate phase space file, which contains energy, position, direction and history for every particle and the thrid stage are described below.

In the first step 6.0×10^9 photons are initiated uniformly throughout the source material region having an isotropic distribution. The source, the source capsule and also primary fixed collimator are included in this step of simulation. The output of this

simulation is energy, position, and directional information of each particle reaching the first scoring plane. That is, the phase space file scored at the first scoring plane just below the primary definer. The total number of particle collected in this scoring plane above secondary collimators is 167396614. The source, the capsule, and the primary collimator do not change by moving or changing the sizes of the secondary collimators for different field sizes. Because of this, it is possible to use this phase space file data for simulation of any field size. Thus, the output of this simulation, the phase space file, is used repeatedly as an input of the next simulation.

The second step of the calculation uses as an input the output of the first step which is the phase space file. This step simulates the passage of the particles through the secondary adjustable collimator, trimmer bars and the air to the plane at which the surface of the phantom or the patient is defined. We simulated different openings of the adjustable outer collimator to get field size from 5 x 5, 10 x 10, 15 x 15, 25 x 25, 30 x 30 cm² at SSD equal to 80 cm. Different number of particle is scored in this stage for different field size at patient plane (at SSD =80 cm)

In the third step of simulation, the phase space files, which are the output of the second stage, for 5 x 5 to 30 x 30 cm² at SSD 80 cm are used by BEAMDP to be analyzed. The data analysis program BEAMDP [3,4] is used to analyze the phase space data files to extract the energy spectra of all photons and electrons reaching at any scoring plane and also the spectra of total scattered photons from the source region and from collimators.

3.2.2 The structure of DOSXYZnrc calculation

All simulations performed here were carried on a water phantom. The output of the BEAMnrc simulation, phase-space data, scored a distance of 80 cm from the ^{60}Co source was, used as a source of particles in the DOSXYZnrc water phantom simulations. Overall phantom dimensions (X,Y,Z) are 30 x 30 x 30 cm³ and with 0.5 x 0.5 x 0.5 cm³ voxels. Particle transport threshold in all DOSXYZnrc simulation are ECUT = 0.521 MeV, PCUT = 0.01 MeV and range of rejection with ESAVE = 2MeV. We used STATDOSE an interactive computer program for 3-dimensional dose, which is the output of DOSXYZnrc, analysis and plotting 1-dimensional dose distributions using the xvgr/xmgr plotting package.

Chapter 4

RESULT AND DISCUSSION

4.1 Effects of field size on photon spectrum

Monte Carlo calculations have been used to study ^{60}Co beams in clinical as well as standard dosimetry laboratory set-ups. Using Monte Carlo simulation different researchers studied ^{60}Co beam from different ^{60}Co radiotherapy units. Here we present energy spectra of total photons and scattered photons from the Theratron equinox 80 ^{60}Co unit at SSD equal to 80 cm for different field size to study effects of changing the field size.

4.1.1 Total photon spectra for different field size

The total photon energy spectra, at the phantom surface, were calculated for different field sizes, and the results are compared figure (4.1) and (4.2). Simulations for field sizes 5 x 5, 10 x 10, 15 x 15, 25 x 25 and 30 x 30 cm^2 were done. The photon energy spectra are calculated in 2 x 2 cm^2 scoring regions. Figure (4.1) compares the photon spectra for 10 x 10 and 30 x 30 cm^2 , and figure (4.2) compares for 15 x 15 and 25 x 25 cm^2 field size. From the two diagrams, the emerging beam from a cobalt treatment machine has a significant component of scattered photon at the patient plane. This is as a result of photon interaction (mostly Compton interaction) with different parts ^{60}Co unit. Therefore, although ^{60}Co decay gives rise to only two gamma-ray lines of 1.17 MeV and

1.33 MeV, the spectrum of photons from the ^{60}Co unit contains a continuum of photon energies as we see in Figure 4.1 and 4.2. Furthermore, both diagrams clearly explain there is a variation in total photon spectra at the phantom surface for different field size. For all cases the fluence of photons is not that much different at lower energies. For energies about 1 MeV the opening collimator or the field size effect is clearly evident in the spectra.

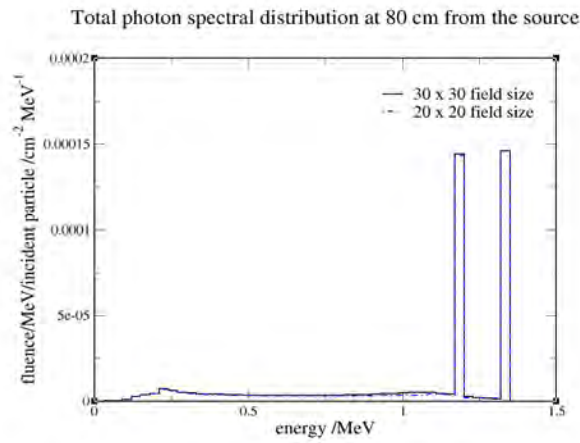


Figure 4.1: Photon energy spectra at the patient plane (SSD=80 cm) for two field sizes (10 x 10, 30 x 30 cm²).

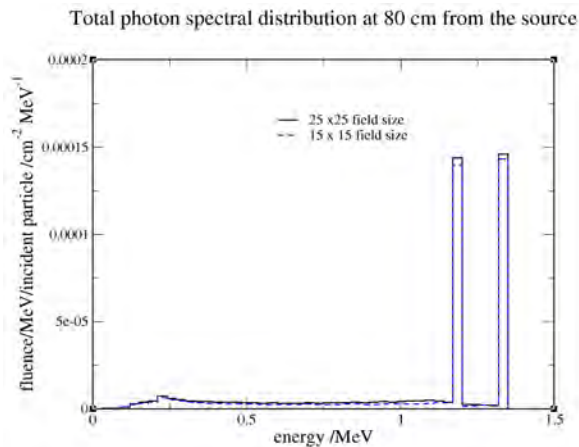


Figure 4.2: Photon energy spectra at the patient plane (SSD=80 cm) for two field sizes (15 x 15, 25 x 25 cm²).

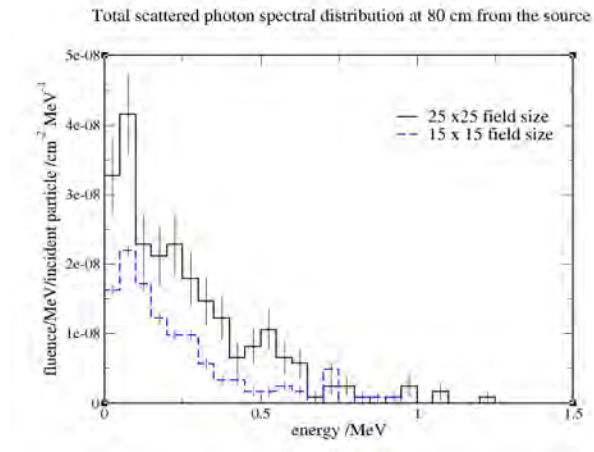


Figure 4.3: Photon energy spectra at the phantom surface: total scattered photon from different components of the therapy unit (excluding primaries), for two field sizes.(15 x 15, 25 x 25 cm²)

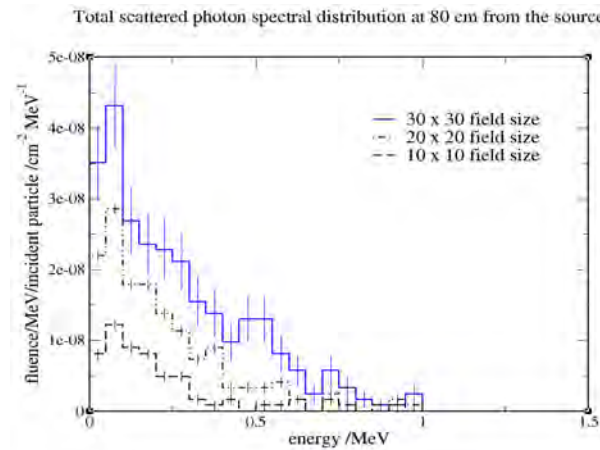


Figure 4.4: Photon energy spectra at the phantom surface: total scattered photon from different components of the therapy unit (excluding primaries), for three field sizes(10 x 10, 20 x 20, 30 x 30 cm²)

4.1.2 Scattered photon spectra for different field size

The total scattered photon energy spectra at the phantom surface, which is scattered from various components of the therapy unit, for different field sizes, are shown in figure (4.3) and (4.4). Figure (4.3) shows the total scattered photon energy spectra for three field sizes (10 x 10, 20 x 20, 30 x 30 cm²) and figure (4.4) shows the total scattered photon energy spectra for two field sizes (15 x 15 and 25 x 25 cm²). The two diagrams

indicate there is a difference in the number of scattered photons for different field size. As the field size gets larger the number of scattered photons increases. This increase in the number of scattered photons arises from the displacement of the adjustable collimator for different field sizes. Thus when the field size changes the number of scattered photons reaching the patient plane, coming from the components of ^{60}Co unit such as source capsule, primary fixed collimator and adjustable collimator also changes. This increase is one of the reasons why the Relative Dose Factor (RDF) for a photon beam increases with an increase in the field size.

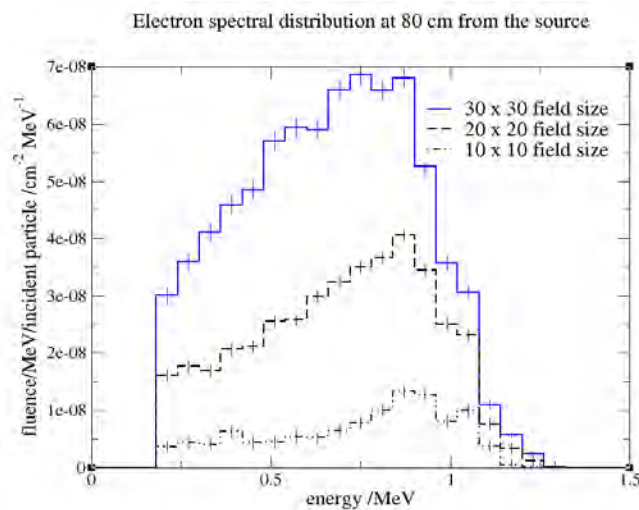


Figure 4.5: Energy spectrum of the electrons reaching at SSD = 80 cm for three field sizes (10 x 10, 20 x 20, 30 x 30 cm²).

4.2 Electron spectra for different field size

In this study we present the electron spectra, which are the product of different interactions of photons with components of the ^{60}Co unit, at the phantom surface for different field size. Figure (4.5) compares electron spectra at the phantom surface (SSD = 80 cm) for three field sizes (10 x 10, 20 x 20, 30 x 30 cm²) and also figure (4.6) compares electron spectra for three field sizes (5 x 5, 15 x 15, 25 x 25 cm²).

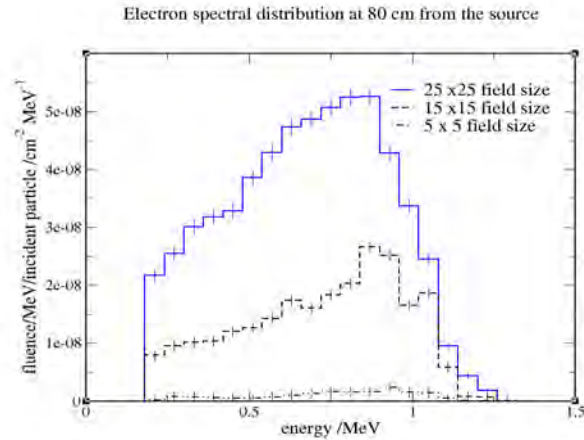


Figure 4.6: Energy spectrum of the electrons reaching at SSD = 80 cm for three field sizes (5 x 5, 15 x 15, 25 x 25 cm²).

We see that the electron fluence increases with field size. From figure (4.5) the electron fluence is about 7 times larger for 30 x 30 cm² beam than the electron fluence for 10 x 10 cm² beam at the patient plane.

4.3 Percentage Depth Dose

In this work, PDDs for two field sizes were calculated. Calculated PDDs, for two different field sizes, 10 × 10, 20 × 20 cm² were compared with the measured values and presented in figure (4.7) and (4.8). The difference between the measured data and calculations were generally less than 1.5 percent and at the worst case it was nearly 3 percent. Therefore, Monte Carlo calculated PDDs for two field sizes 10 x 10, and 20 x 20 cm² show a good agreement with the measured values and properly shows the variation of PDDs with depth along the central axis.

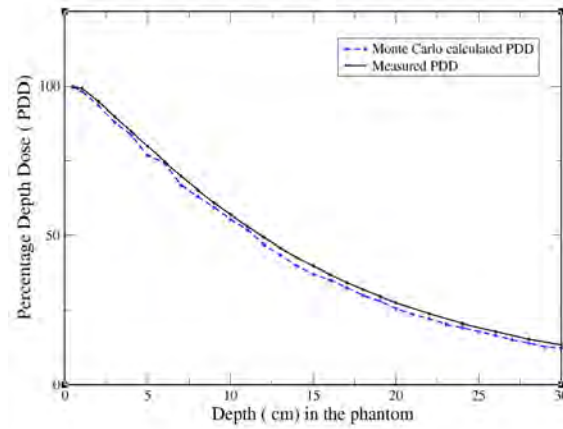


Figure 4.7: Monte Carlo calculation result of percentage depth dose compared with measurement for 10 X 10 cm² field size.

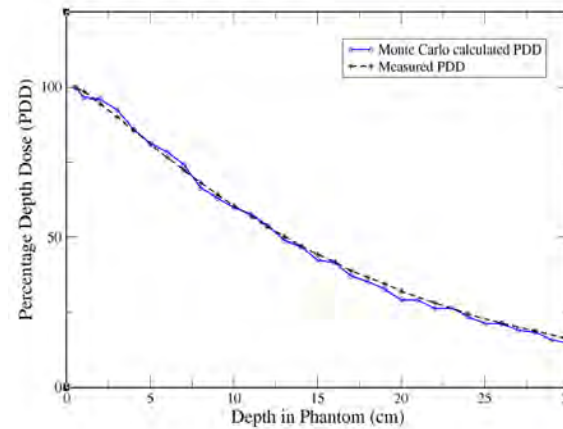


Figure 4.8: Monte Carlo calculation result of percentage depth dose compared with measurement for 20 x 20 cm² field size.

Chapter 5

CONCLUSION

Application of BEAMnrc for the simulation of a ^{60}Co beam from “Theratron equinox 80” radiotherapy unit in this work has produced very promising results. Detailed modeling of the “Theratron equinox 80” radiotherapy machine has resulted in a detailed physical understanding of effects of the field size on energy spectral distribution of the, scattered photons and electrons from different parts of the ^{60}Co unit. Based on our simulation results we were able to conclude that the observed increase in spectral distribution of photons from the ^{60}Co unit with increasing field size is caused by scattered photons from different parts of Cobalt-60 unit. We also observed the increase in energy spectral distribution of electrons (which are produced by interaction of photons) with field size.

In the second part of this thesis we used BEAMnrc generated phase space file at the patient plane, as input source for DOSXYZnrc to score the dose in water phantom. Then we calculated, dosimetric parameter percentage depth dose (PDD) in water phantom and compared with measured values. The Monte Carlo calculated PDD for two field sizes 10 x 10, and 20 x 20 cm^2 show a good agreement with measured values. Therefore, DOSXYZnrc is successfully applied here to score 3-dimensional absorbed dose in water phantom.

Generally the BEAMnrc and DOSXYZnrc Monte Carlo packages have been applied successfully in the simulation of many complicated particle transport problems in radiation therapy sources for applications in dosimetry. Based the results of the simulation of this work, we can conclude that the BEAMnrc and DOSXYZnrc Monte Carlo codes are specifically designed as an effective Monte Carlo simulation packages to carry out a variety of computational dosimetric calculations.

Bibliography

[1] D. W. O. Rogers, B. Walters, and I. Kawrakow. BEAMnrc Users Manual. National Research Council of Canada (NRCC) Report PIRS 0509(A)rev K,2009.

[2] B. R. B. Walters and D. W. O. Rogers. DOSXYZnrc Users Manual. NRCC Report PIRS -794 (rev B) 2009

[3] C.-M. Ma and D. W. O. Rogers. BEAMDP Users Manual. NRCC Report PIRS-0509 (C)rev A

[4] C.-M. Ma and D. W. O. Rogers. BEAMDP as a General-Purpose Utility. NRCC Report PIRS-0509(E)rev A (2009)

[5] J. A. Treurniet and D. W. O. Rogers. BEAMnrc, DOSXYZnrc and BEAMDP GUI User s Manual. NRCC Report PIRS -0623(rev C)

[6] I. Kawrakow and D. W. O. Rogers. The EGSnrc Code System: Monte Carlo simulation of electron and photon transport. Technical Report PIRS 701 (4th printing), National Research Council of Canada(NRC), Ottawa, Canada, 2009.

[7] I. Kawrakow, E. Mainegra-Hing, and D. W. O. Rogers. EGSnrcMP: the multi-platform environment for EGSnrc. Technical Report PIRS 877, National Research Council of Canada, Ottawa, Canada, 2006.

[8] H. C. E. McGowan, B. A. Faddegon, and C-M Ma. STATDOSE for 3D dose distributions. NRC Report PIRS 509(F) (2009)

[9] G. M Mora, A. Maio, and D.W.O Rogers+. Monte Carlo Simulation of a Typical ^{60}Co Therapy Source. Revisions to Med.Phy 99/9/22

[10] D. W. O. Rogers, B. A. Faddegon, G. X. Ding, C.-M. Ma, J. Wei, and T. R. Mackie. BEAM: A Monte Carlo code to simulate radiotherapy treatment units. Med.Phys. 22 (5) May 1995

[11] D. W. O. Rogers, G.M .Ewart, A.F Bielajew. Calculation of Electron Contamination in a ^{60}Co Therapy Beam. From “Proceedings of the Symposium on Dosimetry in Radiotherapy”, Vol 1 (IAEA, Vienna, 1988).

[12] K. Han, D. Ballon, C.Chui, and R. Mohan. Monte Carlo Simulation of a Cobalt-60 beam. Med.Phys. Vol 14 No 3 May/June 1987

[13] B Teimouri Sichani and M Sohrabpour. Monte Carlo dose calculations for radiotherapy machines: Theratron 780-C teletherapy case study. Phys. Med. Biol. 49 (2004) 807818

[14] I. Kawrakowa and B. R. B. Walters. Efficient photon beam dose calculations using DOSXYZnrc with BEAMnrc. Medical Physics, Vol. 33, No. 8, August 2006

[15] D.W.O. Rogers . Monte Carlo Techniques in Radiotherapy (2002) Published in Physics in Canada, Medical Physics Special Issue, 2002 Vol 58 No2, pp 6370

[16] Report of the AAPM Task Group No. 105: Issues associated with clinical implementation of Monte Carlo-based photon and electron external beam treatment planning.

[17] E.B. Podgorsak, Radiation Oncology Physics: A Handbook for Teachers and Students

[18] Harold Elford Johns and John Robert Cunningham, The Physics of Radiology, Fourth Edition

[19] Alex F Bielajew, Fundamentals of the Monte Carlo method for neutral and charged particle transport

Declaration

This thesis is my original work, has not been presented for a degree in any other University and that all the sources of material used for the thesis have been dully acknowledged.

Name: Mesay Geletu

Signature:

Place and time of submission: Addis Ababa University, November. 2010

This thesis has been submitted for examination with my approval as University advisors.

Name: Dr. ERMIAS GETE

Signature:

Name: Dr. MULUGETA BEKELE

Signature: